02-03

16th International Conference on Machine Vision Applications (MVA)
National Olympics Memorial Youth Center, Tokyo, Japan, May 27-31, 2019.

Robust Auto-Calibration for Practical Scanning Setups from Epipolar and Trifocal Relations

Torben Fetzer[1]   Gerd Reis[2]   Didier Stricker[1,2]

[1]Department of Computer Science, University of Kaiserslautern
[2]Department Augmented Vision, DFKI GmbH

{torben.fetzer, gerd.reis, didier.stricker}@dfki.de

Abstract

The most important part of auto-calibration is the estimation of the fundamental matrices and the correction of the distortions caused by optical systems. From the fundamental matrices the state-of-the-art method of Lourakis [17] can determine the intrinsic calibration parameters. The prerequisite is that the fundamental matrices are very accurate, so that subsequent methods can converge. State-of-the-art methods minimize the epipolar error to approximate fundamental matrices. If more than two views are given, the trifocal error can theoretically also be used, but it is very noise sensitive and therefore less practical. In this paper, we propose a combination of both error types that leads to consistently improved fundamental matrices compared to the state of the art. The proposed method has been thoroughly evaluated on both synthetic and real data sets. Besides the increased probability that Lourakis' method converges, the resulting intrinsic and extrinsic parameters are of superior quality. The method is quasi parameter-free, easy to implement, and requires only a slightly increased computational effort.

1 Introduction

The task of calibration is to calculate the intrinsic and extrinsic camera parameters. Basically, there are two types of calibration approaches: On the one hand, methods based on homographies, which exploit additional scene information such as planar structures or calibration tools. On the other hand, auto-calibration methods that allow a calibration of general scenes without user interaction and additional assumptions.

All auto-calibration methods start with the estimation of the fundamental matrices from point correspondences. At the same time, distortion parameters are estimated to account for the underlying pinhole camera model. In further steps intrinsic and extrinsic parameters are extracted from the fundamental matrices. The accuracy of the fundamental matrices is therefore decisive for an exact calibration. Even with slightly inaccurate fundamental matrices, it is likely that the intrinsic calibration and thus the entire calibration process will fail.

In this work we focus on auto-calibration because of its many advantages in practice. The presented procedure uses images from at least three different views. Assuming static scenes, it is basically irrelevant whether these images were taken with several cameras at the same time or one after the other with only one camera. In particular, active lighting elements such as a projector treated as an "inverse" camera can also be considered. In the following, we will therefore limit ourselves to static scenes and use the term View to describe an image content including its pose, completely independent of a point in time or whether an image is captured or projected. We also do not limit the camera settings used for the acquisition. Even if a single camera is used, we do not assume that the camera setting has remained constant for all images. Therefore, shooting is supported with automatic image settings such as auto-focus, as well as the use of different camera models.

The only limitation we make for the observations listed here is that all images reproduce the same scene and largely overlap each other. The calibration can be continued by exchanging the images. All partial calibrations calculated in this way can subsequently be optimized with the help of bundle adjustment.

The approach presented here is the first to combine epipolar and trifocal relations, as well as distortions of arbitrary order. Euclidean reconstruction does not require any information other than the raw image data. For metric calibration it is sufficient to specify a camera baseline or the dimensions of a sensor chip. Since the proposed method is very robust to noise, it provides accurate calibrations in situations where state-of-the-art methods are likely to fail. Especially, no particularly good initialization is required. Thus, the practical applicability of the method is superior to the current state of the art.

2 Related Work

Extensive research has been done in the field of auto-calibration. Estimating the epipolar geometry between two views has been reviewed by Zhang in [27]. In a nutshell, Euclidean epipolar errors between point correspondences are minimized in a nonlinear energy functional. This approach represents the state of the art when distortion-free input images and precise point correspondences are available.

Torr and Zisserman [23] examined the trifocal tensor to derive relationships between three images. Their approach depends on extremely precise point correspondences and is therefore practically unsuitable. Brito et al. [4] and Stein [20] proposed methods to estimate a single radial distortion parameter. Fitzgibbon [9] combined single parameter estimation with the calculation of the epipolar geometry. Unfortunately, this approach is limited because it requires constant intrinsic parameters for all views.

The most advanced distortion model has already been introduced in 1966 by Brown [5] and is still state of the art. Romera and Gomez [19] proposed a method for approximating Brown's distortion parameters using calibration boards for homography estimation.

In the context of auto-calibration, Li et al. [16] presented an alternating method for simultaneously estimating distortions and fundamental matrices, combining the work of Zhang and Brown. Unfortunately, the resulting fundamental matrices are generally not sufficiently accurate to apply Lourakis' [17] state-of-the-art method for further calibration. Gherardi and Fusiello [10] extended this approach, but require very good initialization and the choice of a large number of weighting parameters, which are often not available in practice.

3 Determining the Epipolar Geometry

The calculation of suitable fundamental matrices that meet all expected requirements depends strongly on the quality of the correspondences. Furthermore, since the pinhole camera model is assumed for theoretical consideration, it is crucial to correct distortions of practical systems.

3.1 Background

Relations between the different views are given by fundamental matrices F_{ij} which model the epipolar geometry between image I_i and image I_j. Thereby, fundamental matrix F_{ij} is defined as a rank two matrix that satisfies the condition

$$p_j^\mathsf{T} F p_i = 0, \quad \forall\, p_i \in I_i,\ p_j \in I_j. \qquad (1)$$

Epipolar Error   A standard approach to approximate (1) is to minimize the *epipolar error* for all correspondences and all view pairs. For each point pair
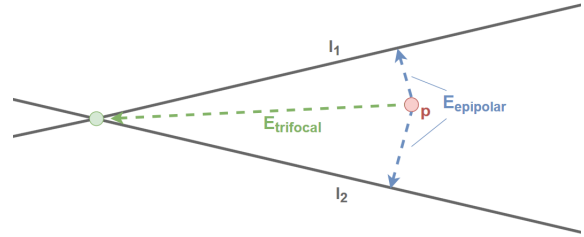

Figure 1. Visualization of E_{epipolar} and E_{trifocal} for an image point p and respective epipolar lines l_1 and l_2 from two other views.

(p_i, p_j) this error is defined by the Euclidean distance of the computed epipolar line $l_{ij} = F_{ij} p_i$ to its respective point p_j in the other image:

$$d(p_j, F_{ij} p_i) = \frac{p_j^\mathsf{T} F_{ij} p_i}{\sqrt{(l_{ij})_1^2 + (l_{ij})_2^2}}, \qquad (2)$$

where $(l_{ij})_1$ and $(l_{ij})_2$ denote the first and second entry of epipolar line l_{ij}. Since this also applies to the mapping F_{ij}^T from p_j to p_i asymmetrically, both errors can be combined to a least squares error by adding the squared distances

$$E_{\text{epipolar}}^{ij} = d(p_j, F_{ij} p_i)^2 + d(p_i, F_{ij}^\mathsf{T} p_j)^2. \qquad (3)$$

This error measure is symmetrical between two views. Considering all epipolar relations between C views, this results in $\frac{C(C-1)}{2}$ epipolar errors.

Trifocal Error   Unlike the epipolar error, which describes only relationships between two views, the *trifocal error* connects relations between three views. For a triple of point correspondences $(p_{i_1}, p_{i_2}, p_j) \in I_{i_1} \times I_{i_2} \times I_j$, theoretically epipolar lines $l_{i_1 j} = F_{i_1 j} p_{i_1}$ and $l_{i_2 j} = F_{i_2 j} p_{i_2}$ should intersect in image point p_j. The squared Euclidean distance between intersection $s_j(l_{i_1 j} \times l_{i_2 j})$ and measured point p_j is defined by

$$E_{\text{trifocal}}^j = \| p_j - s_j(F_{i_1 j} p_{i_1} \times F_{i_2 j} p_{i_2}) \|_2^2, \qquad (4)$$
$$\text{for } (i_1, j),(i_2, j) \in D_2,\ (i_1, j) \neq (i_2, j)$$
$$\text{and } F_{kl} = F_{lk}^\mathsf{T} \text{ for } (k,l) \in D_2 \text{ and } k > l$$

with

$$s_j = ((F_{i_1 j} p_{i_1})_1 (F_{i_2 j} p_{i_2})_2 - (F_{i_1 j} p_{i_1})_2 (F_{i_2 j} p_{i_2})_1)^{-1}. \qquad (5)$$

The set of indices D_2 is given by all combinations of views. For each image we can compute $\frac{(C-1)(C-2)}{2}$ trifocal errors, which leads to $\frac{C(C-1)(C-2)}{2}$ contributions to the total trifocal error.

3.2 Fundamental Matrices

Generally, minimizing the epipolar error is well suited to estimate fundamental matrices between two views. The trifocal error, however, includes a more global arrangement between all views and ensures that all fundamental matrices are coherent. Nevertheless, minimizing the trifocal error usually does not lead to good results as it requires disproportionately good initialization to converge to the global minimum and is sensitive to noisy data. Therefore, a combination of both errors, linked by a scalar regularization parameter $\tau \in \mathbb{R}_0^+$, is introduced to exploit the advantages of both approaches. For a given set of N correspondences in C views, optimal fundamental matrices are sought as the rank two minimizers of functional (6).

$$\underset{\substack{F_{ij} \in \mathbb{R}^{3\times3}, \\ (i,j) \in D_1}}{\operatorname{argmin}} \sum_{n=1}^{N} \sum_{(i,j)\in D_1} E_{\text{epipolar}}^{ij,(n)} + \tau \sum_{j=0}^{C-1} E_{\text{trifocal}}^{j,(n)} \quad (6)$$

$$\text{s.t.} \quad \operatorname{rank}(F_{ij}) = 2, \ \forall(i,j) \in D_1 \quad (7)$$

$E_{\text{epipolar}}^{ij,(n)}$ and $E_{\text{trifocal}}^{j,(n)}$ denote the errors with respect to the n-th point correspondence.

3.2.1 Parameterization of Fundamental Matrices

Since a fundamental matrix has rank two and is up to scale, it has seven degrees of freedom. Following Csurka et al. [7] we parameterize the fundamental matrix according to (8). This parameterization has an optimal condition number, which is important for the convergence rate of the numerical optimization.

$$F(f_1, ..., f_7) = \begin{pmatrix} f_6(f_1f_4 + f_2f_5) \\ +f_7(f_3f_4 + f_5) & f_1f_6 + f_3f_7 & f_2f_6 + f_7 \\ f_1f_4 + f_2f_5 & f_1 & f_2 \\ f_3f_4 + f_5 & f_3 & 1 \end{pmatrix} \quad (8)$$

Minimizing functional (6) under this parameterization enforces property (7).

3.3 Distortion Correction

Due to the least-squares formulation, the quality of a fundamental matrix, computed by minimizing (6), strongly depends on highly accurate point correspondences. Therefore, a distortion correction is essential. According to *Brown's Model* [5], every undistorted image point $\hat{p}$ is related to the observed distorted image point $p = (x, y)^\top$ by

$$\hat{p}(c_d, k_1, ..., k_L) = \begin{pmatrix} c_x + (x - c_x)(1 + \sum_{l=1}^{L} k_l(\frac{r}{d})^{2l}) \\ c_y + (y - c_y)(1 + \sum_{l=1}^{L} k_l(\frac{r}{d})^{2l}) \end{pmatrix} \quad (9)$$

$c_d = (c_x, c_y)^\top$ denotes the center of distortion and $\frac{r}{d} \in [0, 1]$ the Euclidean distance of the normalized distorted image point p to the center of distortion. Taking into account that points p_s are distorted in this way by parameters $c_{d_s}, k_{1_s}, ..., k_{L_s}$ for $s = 1, ..., C$, the distortions can be corrected by minimizing functional (10) assuming fixed fundamental matrices.

$$\underset{\substack{c_{d_s} \in \mathbb{R}^2, k_{l_s} \in \mathbb{R}, \\ l \in \{1, ..., L\}, \\ s \in \{0, 1, C-1\}}}{\operatorname{argmin}} \sum_{n=1}^{N} \sum_{(i,j)\in D_1} E_{\text{epipolar}}^{ij,(n)} + \tau \sum_{j=0}^{C-1} E_{\text{trifocal}}^{j,(n)} \quad (10)$$

3.4 Minimization

In order to obtain the desired epipolar geometry, while correcting the distortions jointly, problems (6) and (10) are alternately minimized. For both sub-problems solutions can be found separately using truncated *Levenberg-Marquardt*, while the variables of the other sub-problem are kept constant. A global solution can finally be found by alternating between both sub-problems.

A good initialization for matrices F_{ij} can be achieved by the *Normalized-Eight-Point* algorithm, possibly combined with RANSAC to account for outliers. For the centers of distortion, the image centers have appeared to be a good initialization for the views. Although the principal point of projectors is generally not in the image center, no special treatment is needed. The radial distortion parameters k_{l_s} are initialized with zeros. Since the center of distortion is usually inside the image, in most cases scaling factor d can be chosen as half of the image diagonal. $N \in \{100, ..., 300\}$ is a good choice for the number of point samples to get accurate results in an acceptable run time.

4 Intrinsic and Extrinsic Calibration

Lourakis et al. [17] introduced a method, based on *Kruppa's equations*, to estimate intrinsic parameters directly from fundamental matrices. Therefore, at least three views are necessary, while more views increase the accuracy as well as the number of calibration parameters that can be estimated. The covariance of the numerical minimization algorithm is used to weight the uncertainties as described in [7] to enhance the stability of the method. Lourakis is state of the art, but requires epipolar relations of high accuracy. Standard techniques (e.g. [27], [16], [10]) for calculating fundamental matrices generally do not provide the quality necessary to estimate intrinsic parameters such as focal length. The method presented in this work solves this problem and provides fundamental matrices of accuracy high enough for precise intrinsic auto-calibration.

With precise fundamental matrices and calibration matrices, extrinsic parameters of the views can be easily extracted, as described in [12], which completes the
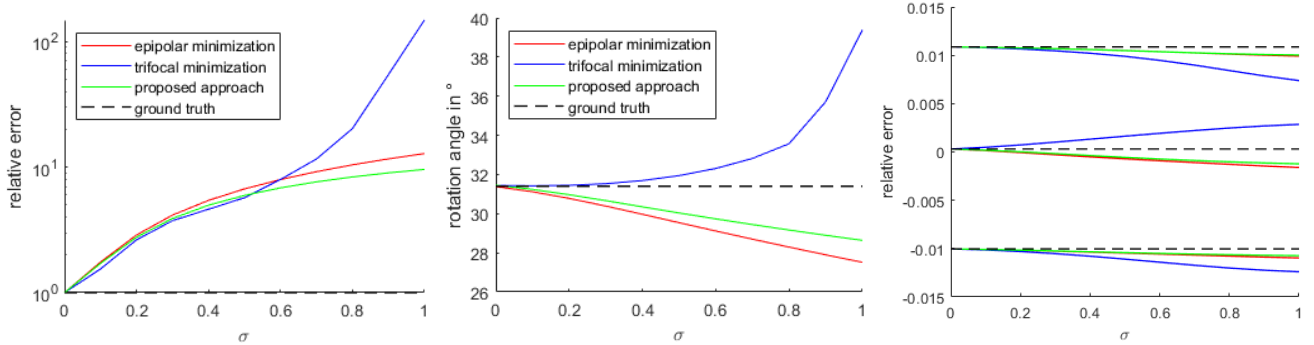
Figure 2. Evaluation on synthetic data for increasing level of Gaussian noise. Back-projection errors (left), angular errors (middle) and distortion coefficients (right) for epipolar, trifocal and the proposed minimization method.

Euclidean auto-calibration. A metric calibration can be inferred if e.g. one of the camera baselines is known. Subsequently, the respective translation vector is simply scaled to the metric value.

5 Evaluation

The proposed method is evaluated to assess its benefits. The effect of regularization parameter τ is examined on real and synthetic data sets. Note that the method for $\tau = 0$ minimizes the epipolar error, while $\tau \to \infty$ is a trifocal minimization. Since the minimization of the epipolar energy term is state of the art [16] and the trifocal error is often not practicable due to its noise susceptibility, we compare the proposed method relative to the pure epipolar minimization.

5.1 Test Data

Both synthetic and real data sets were acquired to evaluate the proposed method. For all data sets, up to 300 correspondences were carefully selected and validated, in order to guarantee absence of outliers. In both cases the same setup, comprised from two cameras and a projection device, has been used. Such a setup is quasi standard for most active scanning solutions and is suitable for evaluation in the contexts of active as well as passive methods.

For the real setup we used DSLR cameras with a resolution of 6M pixels and a full-HD projector. The synthetic setup reproduces the real setup. It was modelled with Unity and has different principal points, various degrees of distortion, and different focal lengths. Apart from that, the synthetic model is a perfect pinhole camera. In order to assess the robustness of the proposed calibration procedure, the synthetic data sets were artificially degraded. To this end, multiple data sets with different levels of positional noise on the correspondences (Gaussian with $\sigma \in [0, 2]$ and $\mu = 0$) were derived. On this data, the back-projection error as well

as the angular error with respect to the cameras were computed (see Figure 2).

For evaluation of the real data, a calibration with several values for the regularization parameter $\tau \in [10^{-6}, 10^{4}]$ was calculated. After computing the calibration, the remaining epipolar as well as trifocal error were estimated (see Figure 3).

5.2 Results

Using the synthetic data we observe that:

- For noise-free data the selection of τ is irrelevant, since both error terms converge robustly to the global minimum. (See Figure 2 for $\sigma = 0$). Also the proposed combination provides the expected result.

- For slightly noisy data ($\sigma < 0.5$) the trifocal error clearly outperforms epipolar optimization. Although the proposed method is not better than the trifocal minimization, it consistently outperforms the state of the art (See Figure 2).

- For very noisy data ($\sigma > 0.5$), minimizing the trifocal error does not provide useful results. In this case, minimizing the epipolar error is much more robust and yields stable results. The same is true for the proposed method, which consistently provides significantly better results than the state of the art.

The proposed combination of both errors improves the state of the art (i.e. epipolar optimization) for all cases with $\sigma > 0$. Figure 2 gives an impression of the relation between noise and errors. In terms of the back-projection error (left), the improvement is up to 30% with respect to the state of the art. In terms of angular error (middle), we observe an improvement of 1-2 degrees. This is equivalent to a 3D point position error of not less than 1.7cm assuming a baseline of 1m.
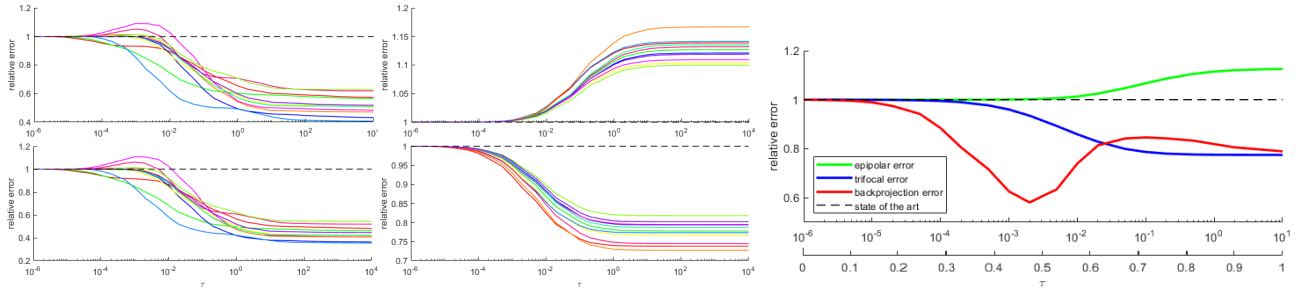
Figure 3. Mean epipolar error (top left, top middle) and mean trifocal error (bottom left, bottom middle) computed from high quality (left) and noisy (middle) real data sets. Average errors from real data sets with different noise levels (right).

To evaluate the accuracy of the distortion parameters computed by the proposed method, we have generated distorted synthetic data using Unity. An example for simultaneous distortion parameters (-0.01, 0.0005, 0.011) is given in Figure 2 (right). Unfortunately, the parameter space under investigation is too large to allow extensive evaluation. We have therefore focused on the evaluation of the first coefficient of the distortion model, since it dominates the others and reflects the majority of distortions caused by lenses. Gaussian noise of $\sigma \in [0, 1]$ was applied to investigate the influence of measurement errors. Figure 2 (right) shows the estimated radial distortion coefficients for increasing values of σ. We observe that all methods provide useful distortion parameters. The proposed method provides consistently superior parameters, although the improvement may be marginal.

5.2.1 Choice of Regularization Parameter τ

In Figure 3 all errors are given relative to the state of the art ($\tau = 0$), i.e. pure epipolar error optimization. On the left side, the behavior of the mean epipolar error (top) and the mean trifocal error (bottom) is visualized. In total 100 uncorrelated data sets have been investigated, using 300 high quality correspondences respectively. By emphasizing the trifocal term, both the trifocal error as well as the epipolar error are improved.

Figure 3 (middle) visualizes the behavior of the errors after adding weak Gaussian noise ($\sigma = 0.3$). We observe that the minimization of the trifocal error in the presence of noise does not lead to lower epipolar errors, but the epipolar error increases significantly ($> 10\%$). Hence, adding a small amount of noise dramatically reduces the dependency (see Figure 1) between the epipolar and the trifocal error.

Since neither of the two errors is to be preferred in principle, a combination of both errors is well reasoned. Another suitable measure for the calibration quality is the back-projection error. Applying the proposed method, similarly to the previous section, to 100 uncor-

related data sets with different noise levels, results in average errors visualized in Figure 3 (right). Minimal back-projection errors were achieved with a selection of $\tau = 10^{-3}$ over a large number of data sets. Therefore, it can be assumed that τ is a constant, rendering the proposed method quasi parameter-free. Note that trifocal errors are usually much larger than epipolar errors, a value of $\tau = 10^{-3}$ leads to nearly equal influence of both errors to the minimization. In Figure 3 (right) we show the original value of τ according to (6) in the upper ordinate. The lower ordinate shows τ after a transformation into the interval $[0, 1]$ using normalized energies.

6 Conclusions

A new method for robust computation of highly accurate calibration of multiple views (i.e. cameras and projectors) has been proposed and evaluated. The method combines the advantages of epipolar and trifocal approaches and eliminates many weaknesses, especially in the presence of noisy data. The method consistently outperforms the state of the art with respect to both, positional and angular error as well as the back-projection error. A suitable regularization parameter τ has been estimated and fixed, so that the resulting method can be assumed parameter-free. We observe that the optimal result is achieved when epipolar and trifocal errors contribute about the same amount to the calibration. The resulting fundamental matrices are of very high quality and increase the probability that state-of-the-art methods for intrinsic calibration (e.g. Lourakis [17]) converge. Finally, the method is easy to implement and needs only marginally increased computational effort.

References

[1] S. Agarwal, N. Snavely, S. M. Seitz, and R. Szeliski. Bundle adjustment in the large. In *European conference on computer vision*, pages 29–42. Springer, 2010.

[2] J. P. Barreto and K. Daniilidis. Fundamental matrix for cameras with radial distortion. In *Computer Vision, 2005. ICCV 2005. Tenth IEEE International Conference on*, volume 1, pages 625–632. IEEE, 2005.

[3] S. Bougnoux. From projective to euclidean space under any practical situation, a criticism of self-calibration. In *Computer Vision, 1998. Sixth International Conference on*, pages 790–796. IEEE, 1998.

[4] J. H. Brito, R. Angst, K. Köser, and M. Pollefeys. Radial distortion self-calibration. In *Computer Vision and Pattern Recognition (CVPR), 2013 IEEE Conference on*, pages 1368–1375. IEEE, 2013.

[5] D. C. Brown. Decentering distortion of lenses. *Photogrammetric Engineering and Remote Sensing*, 1966.

[6] M. Byrod, Z. Kukelova, K. Josephson, T. Pajdla, and K. Astrom. Fast and robust numerical solutions to minimal problems for cameras with radial distortion. In *Computer Vision and Pattern Recognition, 2008. CVPR 2008. IEEE Conference on*, pages 1–8. IEEE, 2008.

[7] G. Csurka, C. Zeller, Z. Zhang, and O. D. Faugeras. Characterizing the uncertainty of the fundamental matrix. *Computer vision and image understanding*, 68(1):18–36, 1997.

[8] O. Faugeras. Stratification of three-dimensional vision: projective, affine, and metric representations. *JOSA A*, 12(3):465–484, 1995.

[9] A. W. Fitzgibbon. Simultaneous linear estimation of multiple view geometry and lens distortion. In *Computer Vision and Pattern Recognition, 2001. CVPR 2001. Proceedings of the 2001 IEEE Computer Society Conference on*, volume 1, pages I–I. IEEE, 2001.

[10] R. Gherardi and A. Fusiello. Practical autocalibration. In *European Conference on Computer Vision*, pages 790–801. Springer, 2010.

[11] R. Hartley. Extraction of focal lengths from the fundamental matrix. *Unpublished manuscript*, 1993.

[12] R. Hartley and A. Zisserman. *Multiple view geometry in computer vision*. Cambridge university press, 2003.

[13] R. I. Hartley. Kruppa's equations derived from the fundamental matrix. *IEEE Transactions on pattern analysis and machine intelligence*, 19(2):133–135, 1997.

[14] Z. Kukelova, J. Heller, M. Bujnak, A. Fitzgibbon, and T. Pajdla. Efficient solution to the epipolar geometry for radially distorted cameras. In *Proceedings of the IEEE international conference on computer vision*, pages 2309–2317, 2015.

[15] Y.-t. Kwak, J.-w. Hwang, and C.-j. Yoo. A new damping strategy of levenberg-marquardt algorithm for multilayer perceptrons. *Neural Network World*, 21(4):327, 2011.

[16] F. Li, H. Sekkati, J. Deglint, C. Scharfenberger, M. Lamm, D. Clausi, J. Zelek, and A. Wong. Simultaneous projector-camera self-calibration for three-dimensional reconstruction and projection mapping. *IEEE Transactions on Computational Imaging*, 3(1):74–83, 2017.

[17] M. I. Lourakis and R. Deriche. *Camera self-calibration using the singular value decomposition of the fundamental matrix: From point correspondences to 3D measurements*. PhD thesis, INRIA, 1999.

[18] M. Pollefeys, R. Koch, and L. Van Gool. Self-calibration and metric reconstruction inspite of varying and unknown intrinsic camera parameters. *International Journal of Computer Vision*, 32(1):7–25, 1999.

[19] L. Romero and C. Gomez. Correcting radial distortion of cameras with wide angle lens using point correspondences. In *Scene Reconstruction Pose Estimation and Tracking*. InTech, 2007.

[20] G. P. Stein. Lens distortion calibration using point correspondences. In *Computer Vision and Pattern Recognition, 1997. Proceedings., 1997 IEEE Computer Society Conference on*, pages 602–608. IEEE, 1997.

[21] P. Sturm. On focal length calibration from two views. In *Computer Vision and Pattern Recognition, 2001. CVPR 2001. Proceedings of the 2001 IEEE Computer Society Conference on*, volume 2, pages II–II. IEEE, 2001.

[22] G. Terzakis, P. Culverhouse, G. Bugmann, S. Sharma, and R. Sutton. A recipe on the parameterization of rotation matrices for non-linear optimization using quaternions. Technical report, Technical report MIDAS. SMSE. 2012. TR. 004, Marine and Industrial Dynamic Analysis School of Marine Science and Engineering, Plymouth University, 2012.

[23] P. H. Torr and A. Zisserman. Robust parameterization and computation of the trifocal tensor. *Image and vision Computing*, 15(8):591–605, 1997.

[24] B. Triggs, P. F. McLauchlan, R. I. Hartley, and A. W. Fitzgibbon. Bundle adjustmenta modern synthesis. In *International workshop on vision algorithms*, pages 298–372. Springer, 1999.

[25] A. Whitehead and G. Roth. Estimating intrinsic camera parameters from the fundamental matrix using an evolutionary approach. *EURASIP Journal on Advances in Signal Processing*, 2004(8):412751, 2004.

[26] Z. Zhang. On the epipolar geometry between two images with lens distortion. In *Pattern Recognition, 1996., Proceedings of the 13th International Conference on*, volume 1, pages 407–411. IEEE, 1996.

[27] Z. Zhang. Determining the epipolar geometry and its uncertainty: A review. *International journal of computer vision*, 27(2):161–195, 1998.